Bioorganic Chemistry 91 (2019) 103139

Contents lists available at ScienceDirect

Bioorganic Chemistry

journal homepage: www.elsevier.com/locate/bioorg

Water soluble thioglycosylated BODIPYs for mitochondria targeted cytotoxicity

Praseetha E. Kesavan[a], Vijayalakshmi Pandey[a], Md Kausar Raza[b], Shigeki Mori[c], Iti Gupta[a,*]

[a] Indian Institute of Technology Gandhinagar, Palaj Campus, Gandhinagar, Gujarat 382355, India
[b] Department of Inorganic and Physical Chemistry, Indian Institute of Science, Bangalore 560012, India
[c] Integrated Centre for Sciences, Ehime University, Matsuyama 790-8577, Japan

ARTICLE INFO

Keywords:
Thioglycosylated BODIPY
Fluorescence imaging
Mitochondria targeting
Water soluble BODIPYs

ABSTRACT

The facile synthesis of water-soluble mitochondria targeting thioglycosylated BODIPYs is reported. Thioglycosylated BODIPYs were synthesized in 25–26% yields via thioglycosylated dipyrromethanes in four steps. The dipyrromethanes and thioglycosylated BODIPYs were characterized by various techniques including HRMS, NMR spectroscopy and X-ray crystallography. *In-vitro* cellular investigations in skin keratinocyte (HaCaT) and cervical (HeLa) cancer cells revealed significant cytotoxicities with IC_{50} values between 23.83 to 48.61 μM. The flow cytometry experiments revealed significant cellular uptake of thioglycosylated BODIPYs into HaCaT cells and thioglucosyl substituted BODIPY (**9**) showed higher cellular uptake and ROS generation than the rest of the molecules. The highlight of this study is the mitochondrial targeting by the neutral BODIPYs, as judged by the colocalization experiments using confocal microscopy.

1. Introduction

Fluorescence imaging technique is one of the highly useful and powerful methods to monitor and visualize bioprocesses and targets in real time [1]. Because of its operational simplicity, high sensitivity and specificity, this imaging technique is adapted for various areas of research in biological sciences [2]. This non-invasive method for cellular imaging depends on the stable and specific fluorescent probes. BODIPY (BF_2 complex of dipyrromethene) is a class of highly fluorescent dyes with strong absorption, high molar extinction coefficients and bright emission in visible to near IR (infrared) region. High quantum yields, long fluorescence lifetimes, good photostability, low toxicity [3] and reasonable Stokes' Shifts [4,5] made this molecule prevalent candidate for biological applications. BODIPYs are widely used as fluorescent tags to label proteins and the DNA, and as photosensitizers in PDT [6]. BODIPYs substituted with appropriate functionality are employed as chemosensors to bind toxic heavy metals [7], anions [8], proteins (BSA and Tau) [9,10] and for reactive oxygen species (ROS) generation [11]. BODIPY derivatives have been demonstrated as promising agents for *in-vivo* fluorescence imaging in the fields of diagnosis and bioanalysis. Cellular organelles like mitochondria and endoplasmic reticulum (ER) are found in most of the eukaryotic cells and play key roles in many cellular processes related to cell survival and death [12]. Mitochondria not only provide energy to the cells by generating ATP; they are also responsible for initiating cell apoptosis, producing cellular ROS, regulating cell proliferation and the cell cycle [13]. Mitochondria have significant roles in regulating the cell metabolism and any damage or disorder in mitochondria can lead to serious human diseases such as: cancer, autism [14], cardiovascular dysfunction [15] and multiple endocrinopathy [16]. Therefore, considerable efforts are dedicated to study the abnormal functions of mitochondria in biomedical research [17,18]. However, large number of cellular activities, mitochondrial functions and related mechanisms are still unclear. In order to track morphology and subcellular localization of mitochondria, a fluorescent probe should have certain characteristics such as: (a) considerable photostability, (b) water solubility, (c) strong emission and reasonable fluorescence quantum yield in aqueous media, (d) Specific targeting to mitochondria and (e) high binding affinity for mitochondria [19]. A variety of commercially available fluorescent probes used for mitochondrial imaging includes cyanine dyes [20], rhodamine derivatives [21] and Mito-Tracker series. Still, such dyes have limitations like low selectivity, photo-bleaching and hindering mitochondrial respiration [22]. Majority of the reported cationic probes are chemically unstable and they induce cytotoxicity by imposing mitochondrial membrane depolarization, which limits their applications [23]. Thus, neutral or noncationic mitochondrial probes are in demand. A recent report suggested that neutral fluorescent molecules having strong electron acceptor groups are promising candidates for mitochondrial targeting in

* Corresponding author.
E-mail address: iti@iitgn.ac.in (I. Gupta).

https://doi.org/10.1016/j.bioorg.2019.103139
Received 15 November 2018; Received in revised form 10 July 2019; Accepted 19 July 2019
Available online 23 July 2019

live cells [19]. Neutral BODIPY derivatives can also be good substitute of the reported cationic probes to target mitochondria [23]. The hydrophobic nature of BODIPYs can be altered by substituting water soluble groups on the molecular framework. Covalent linking of phosphonates [24], (oligoethyleneglycol) chains, sulfonates, carboxylate, sulfonated peptides and alkoxy groups on the BODIPY core are some of the successful strategies to prepare hydrophilic BODIPY dyes in good yields [25]. Also, the linkage of hexose sugars to BODIPY scaffold can easily afford water-soluble fluorescent probes [26]. The substitution of hexose sugar at α-methyl position(s) of pyrrole ring is reported to enhance the hydrophilicity of the BODIPYs [27]; additionally, the presence of hexose sugar can also expedite cell uptake of the fluorophore.

In this work, we report a facile synthetic route to prepare water soluble thioglycosylated BODIPYs. These BODIPYs were synthesized from thioglycosylated dipyrromethanes in decent yields and characterized by different techniques including HRMS, IR, NMR, UV–vis absorption and fluorescence spectroscopy. Single crystal X-ray structure of thiogalactoside linked BODIPY (**6**) is also presented. The water soluble BODIPYs exhibited moderate cytotoxicity in HeLa and HaCaT cancer cells which originated from the reactive oxygen species and they revealed significant cellular uptake of BODIPYs in live cells as indicated by flow cytometric analysis. Fluorescent microscopy colocalization experiments demonstrated the ability of these neutral thioglycosylated BODIPYs to target mitochondria in live cells for bioimaging.

2. Results and discussion

2.1. Synthesis

The synthetic strategy to prepare thioglycosylated BODIPYs is shown in Scheme 1. Firstly, thioglycosylated dipyrromethanes (**4** and **5**) were prepared by reacting the meso-penta-fluorophenyl-dipyrromethane with 2,3,4,6-tetra-*O*-acetyl-β-D-thiagalactopyranose or 2,3,4,6-tetra-*O*-acetyl-β-D-thiaglucopyranose in DMF [28]. Silica gel column chromatography afforded thioglycosylated dipyrromethanes **4** and **5** in excellent yields (85%). Compunds **4** and **5** are the novel key precursors, which can be utilized further to synthesize BODIPYs and/or porphryins bearing thiogalactose or thioglucose moieties. Compounds **4** and **5** were dissolved in dichloromethane (DCM) and oxidized with 2,3-dichloro-5,6-dicyano-1,4-benzoquinone (DDQ) for 30 min; then triethyl amine and $BF_3.OEt_2$ were added into the reaction. Desired glycosylated BODIPYs **6** and **7** were obtained after silica gel column chromatography in 35 and 37% yields, respectively. The water-soluble derivative of BODIPYs **6** and **7** were prepared by deprotecting the acetyl groups of sugar in the presence of base; amberlyst treatment afforded thioglycosylated BODIPYs **8** and **9** in 25–26% yields. All the compounds were characterized using IR, ^{1}H NMR, ^{13}C NMR and mass spectrometry (Supporting Information, S3–S14). The ^{11}B NMR of BODIPYs **6** and **7** showed triplet around 0.05–0.40 ppm due to the coupling of boron with adjacent fluorine nuclei (Fig. 1). The ^{19}F NMR of BODIPYs **6** and **7** showed three set of signals (Fig. 1). The ^{19}F peak at −129 and −136 ppm are due to the four fluorine atoms of the meso-aryl ring.

The peak around −144 ppm corresponds to the two fluorine atoms attached to boron in the BODIPYs. The ^{19}F NMR pattern clearly confirmed the substitution of one fluorine atom of *penta*-fluorophenyl ring by thioglycosyl group in the BODIPYs. The X-ray crystal structure of glycosylated BODIPY **6** was analysed. The orange colour crystals were obtained by slow evaporation of hexane diffused in DCM. The single crystals of BODIPY **6**, showed monoclinic system with $P2_1$ space group (Fig. 2). The central boron dipyrrin core is planar in compound **6**. It is clear from the figure that, the *penta*-fluorophenyl unit, thioglycosyl unit and boron dipyrrin core are not aligned in the same plane. In BODIPY **6**, the dihedral angle [C6-C5-C10-C11] between glycosylated *tetra*-fluorophenyl ring and boron dipyrrin plane is 58.89°(4); which is comparable with the reported meso-phenyl BODIPY (reported value is 60°). The thioglycosyl unit is attached to *tetra*-fluorophenyl ring through sulphur atom [C13-S1-C16] has a bond angle of 95.85°(14).

2.2. Absorption and emission properties

The UV–Vis absorption and fluorescence studies of thioglycosylated BODIPYs **6** and **7** were carried out in methanol (Fig. 3, Table 1). Molar extinction coefficients corresponding to the major absorption band of these molecules were between 23,000 and 26,400 $M^{-1}\,cm^{-1}$.

The absorption spectra of BODIPYs **6–9** (Fig. 3) showed two bands, the longer wavelength band centred at ~513 nm corresponds to the $S_0 \rightarrow S_1$ transition. Whereas, the shorter wavelength band with absorption maximum at ~340 nm was assigned to the $S_0 \rightarrow S_2$ transition in the molecules [29]. The BODIPYs **6–9** exhibited emission maxima ~536 nm in methanol with moderate fluorescence quantum yields around 0.35. The maximum Stoke's shift observed for these molecules is 24 nm.

2.3. Lipophilicity

In order to gauge the membrane permeability and the probability of BODIPYs (**8** and **9**) to distribute between hydrophilic and hydrophobic cellular pockets, Log P values were calculated by shake-flask method [30]. In this shake flask method compounds **8** and **9** were partitioned between the two layers of 1-octanol and PBS (phosphate buffered saline) and their optical densities were measured and Log P values were determined. In general, compounds with lipophilicity between 1 and 3 have shown good membrane permeability; for water soluble BODIPYs **8** and **9** the calculated Log P values were 2.5 and 1.9, respectively. The observed Log P values of **8** and **9** are comparable to the previously reported mono-alkoxy BODIPYs [30], making them suitable candidates for biological applications.

2.4. Cytotoxicity studies

Cell viability of BODIPYs (**6–9**) was evaluated by standard MTT assay [31] using HaCaT and HeLa cells (Fig. 4, Table 2). Both types of cells were incubated with varying concentrations of BODIPYs (**6–9**) (3.1–100 μM) for 24 h.

The half maximal inhibitory concentrations (IC_{50} values) [27] represent the concentrations of the dyes required to kill 50% of the cells; and the IC_{50} values for BODIPYs **6–9** in both HaCaT and HeLa were found to be 23.83–48.61 μM. Furthermore, higher concentrations (50–100 μM) of **6–9** instigated significant cellular damage, suggesting that glycosylated BODIPYs **6–9** can potentially be used for cancer therapy in future. The IC_{50} values of the BODIPYs **6–9** in HaCaT cells were in the range of 23.83–38.15 μM; and between 29.51 to 48.61 μM in HeLa cells; these values are comparatively lower than the reported non-glycosylated BODIPYs. The cell viability data reveal that the deprotected glycosylated BODIPYs **8** and **9** are cytotoxic in comparison to protected glycosylated BODIPY **6** and **7** in both HaCaT and HeLa cells respectively.

2.5. Cellular uptake and ROS generation

Generally, the proliferating cancer cells are under more oxidative stress than the normal cells, due to their high metabolic rates. Mitochondria are imperative for energy metabolism as they synthesize most of the cellular ATP through oxidative phosphorylation. Generally, cancer cells have altered mitochondrial oxidative metabolism and enhanced lactate production; known as "Warburg effect" [32]. An enhanced glucose uptake and/ or a down regulation of mitochondrial metabolism are alleged to be associated with "Warburg effect". This effect is supported by the observed overexpression of high affinity glucose transporters (Glut1 and Glut3) in several cancer cell lines [33]. Previous report on hepatocarcinoma and HeLa cell lines suggested that, glucose transport affects the glycolysis process; and thus, it can be

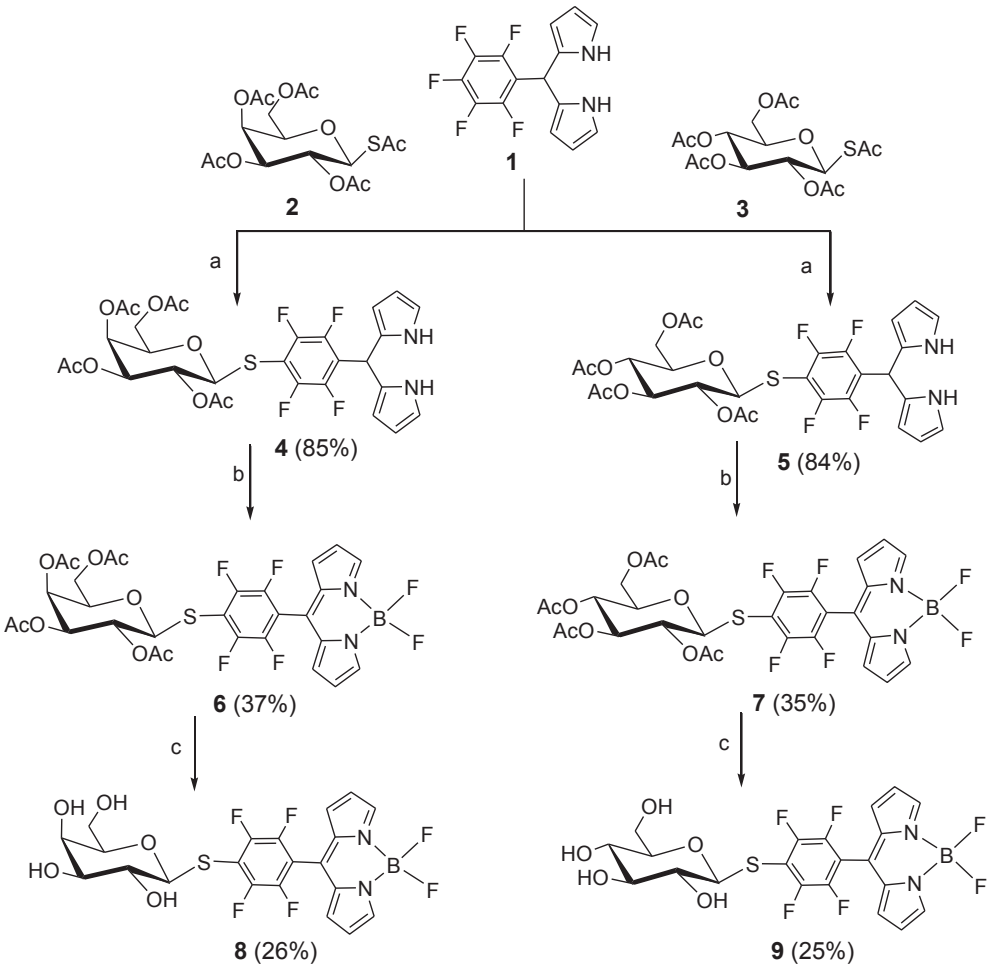

Scheme 1. Synthesis of glycosylated BODIPYs; (a) DMF, DEA, 12 h, RT; (b) DCM, $BF_3.OEt_2$, TEA, 2 h, RT; (c) $CHCl_3$/MeOH, NaOMe, Amberlyst, 16 h, RT.

suitable target for anti-tumor agents [34]. Moreover, studies have shown that the ROS, such as hydrogen peroxide (H_2O_2) and superoxide anions (O_2^-) are generated as by-products of respiration and play important role in mitochondrial dysfunction during apoptosis. The cell cytotoxicity experiments indicated that the glycosylated BODIPYs were more active in HaCaT cells as compared to the HeLa cells (Table 2); thus, flow cytometry analysis was carried out with HaCaT cells to understand the cellular uptake of BODIPYs **6–9** (Fig. 5).

As expected, the deprotected glycosylated BODIPYs **8** and **9** are having higher cellular uptake compared to their corresponding protected glycosylated BODIPYs **6** and **7**; this could be the reason for higher cytotoxicity of deprotected glycosylated BODIPYs than the protected glycosylated BODIPY analogues. Furthermore, the thioglucosyl BODIPY (**9**) showed highest cellular uptake compared to the thiogalactosyl BODIPY (**8**). To evaluate the reason for the cytotoxicity of BODIPYs **6–9**, DCFDA assay was carried out as the reactive oxygen species (ROS) play important role to induce apoptotic cell death [35]. DCFDA is cell permeable molecule and upon oxidation by cellular ROS, it generates the fluorescent DCF, which has emission maxima at 528 nm. The HaCaT cells were incubated with BODIPYs **6–9** (20 μM) for 24 h and the ROS generation properties was determined by flow cytometry analysis (Supporting Information, Fig. S2). The BODIPYs **6** and **7** with acetylated hexose sugar moieties exhibited smaller shifts in the band as compared to the band shown by only DCFDA treated cells or with the compounds **8** and **9** treated cells. On the other hand, BODIPYs **8** and **9** with deprotected hexose sugar moieties experienced significant

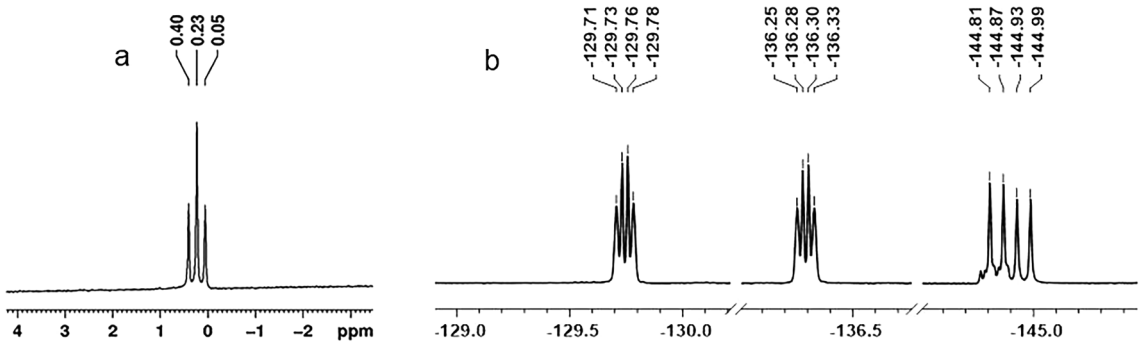

Fig. 1. (a) ^{11}B NMR and (b) ^{19}F NMR spectra of BODIPY **7** recorded in $CDCl_3$.

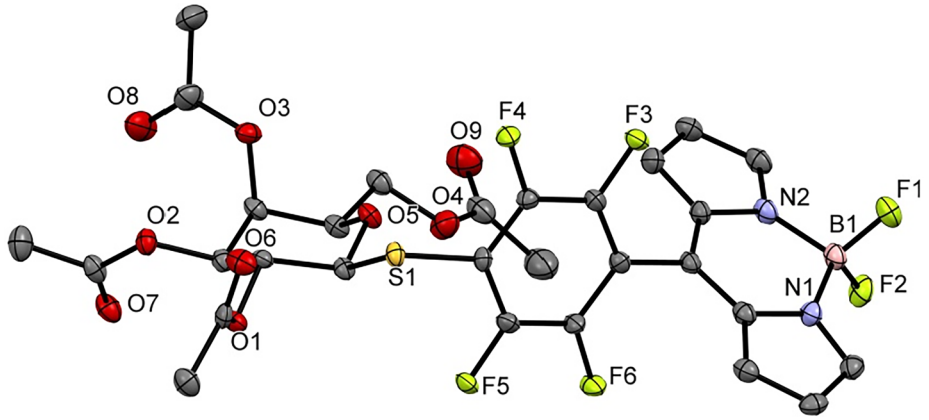

Fig. 2. ORTEP diagram of the X-ray crystal structure of BODIPY **6**, thermal ellipsoids are shown at 50% probability level, H atoms are omitted for clarity.

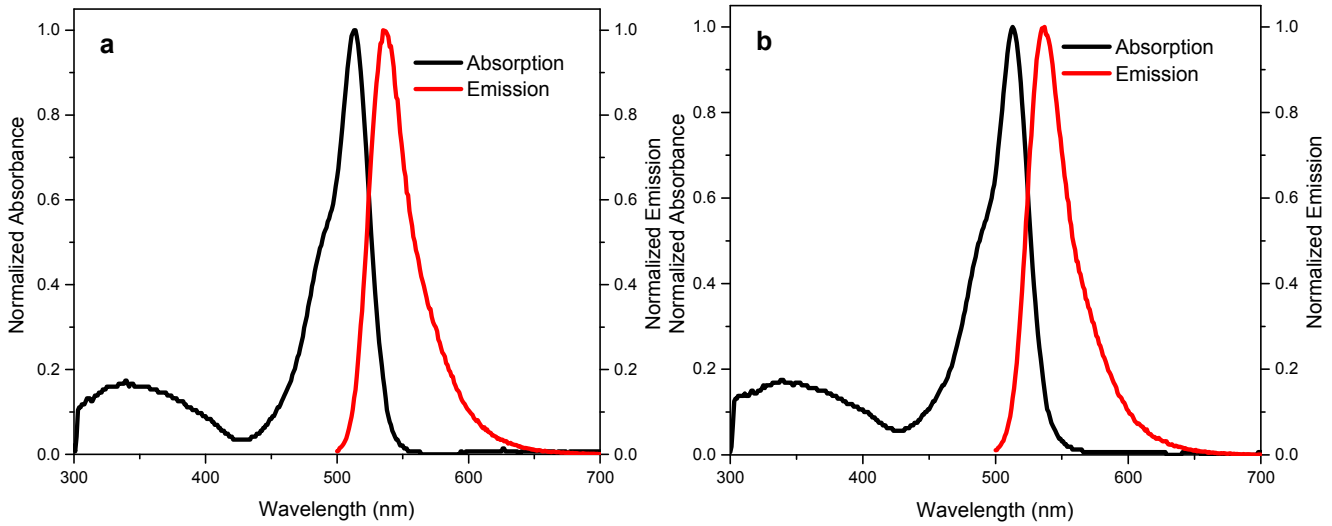

Fig. 3. Comparison of absorption and emission spectra of (a) BODIPY **8**; (b) BODIPY **9** in methanol.

Table 1
Absorption and emission data of glycosylated BODIPYs **6–9** in methanol.

Compounds	λ_{abs} (nm)	ε (M^{-1} cm^{-1})	λ_{em} (nm)	Stokes shift (cm^{-1})	ϕ_f[a]
6	514	23,600	536	798	0.35
7	513	26,400	537	871	0.33
8	513	23,200	535	802	0.36
9	513	26,000	537	871	0.33

[a] Rhodamine 6G was used as reference (ϕ_f = 0.95 in EtOH), λ_{ex} = 488 nm.

shift in the band as compared to the band corresponding to DCFDA treated cells. Overall, BODIPY **9** substituted by thioglucosyl unit showed maximum ROS generation.

2.6. Mitochondrial localization

Recent studies have suggested that, mitochondria can be potential targets for anticancer therapy as they play significant role in cell death. The mitochondrial-targeted drugs can trigger apoptosis in tumour cells and shown to suppress the growth of various types of carcinomas in animal models. Thus, fluorescent probes designed for mitochondrial targeting have gained much attention in recent years [36]; bifunctional BODIPYs having mitochondrial-targeting TPP^+ (triphenylphosphinium) and/ or pyridinium moieties were capable to show *in-vitro* anticancer activity and efficient subcellular imaging in live cells [37,38]. The viscosity of the mitochondrial matrix is also linked to the respiratory state of the mitochondria; and the cationic coumarin-BODIPY conjugate has been reported by Kang et al. to investigate intracellular viscosity in live cells [39]. The coumarin-BODIPY conjugate containing TPP cation was preferentially localized in mitochondria and it was useful to monitor the changes in mitochondrial viscosity. Murphy et al. have reported the cationic BODIPY substituted with diene (a peroxidation sensitive group) and TPP^+ (mitochondria targeting unit) [40]; the cell permeable fluorescent probe displayed enhanced emission around 520 nm with significant staining of mitochondria in live cells. The NIR fluorescent probes based on carbazole-BODIPY conjugate [41] and aza-BODIPY containing TPP cation (for selective imaging of mitochondria) were also developed [42], latter was used for the detection of mitochondrial hydrogen polysulfides. Z. Xie and co-workers reported the pyridyl substituted BODIPY-platinum conjugate [43]; the probe displayed considerable cytotoxicity towards HeLa and MCF-7 cancer cells with IC_{50} values 27.37 and 12.14 μM, respectively.

The excellent photophysical properties of BODIPY dyes and organelle targeting properties lead us to investigate their cellular tracking. The thioglycosylated BODIPYs **8** and **9** (10 μM) incubated for 24 h in HaCaT cells using 5% DMSO/DMEM buffer. The intracellular distribution of compounds **8** and **9** was observed through colocalization imaging technique (Fig. 6). The HaCaT cells were incubated with a nuclear staining dye DAPI (4′,6-diamidino-2-phenylindole) and thioglycosylated BODIPYs **8** or **9**; the merged images displayed cytoplasmic localization of the probes (Fig. 6). The subcellular colocalization of BODIPYs **8** and **9** was further evaluated with MTR (Mito Tracker Deep Red)

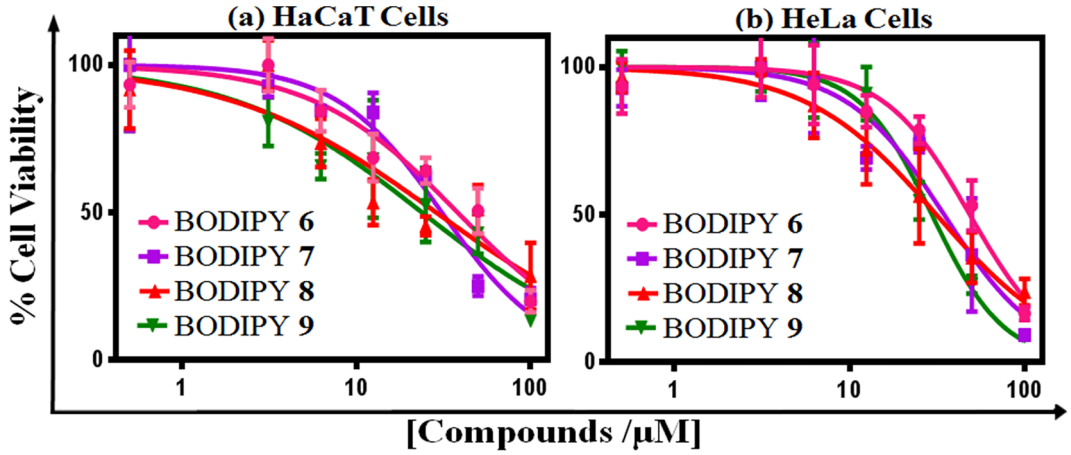

Fig. 4. Cell viability plots as obtained from MTT assay in cancer cells treated with BODIPY **6–9** for 24 h.

Table 2
Comparative cytotoxicity of the BODIPYs **6–9.**

Compounds	IC_{50}[a] (μM)	
	HaCaT cells	HeLa cells
6	38.15 ± 1.6	48.61 ± 1.4
7	30.98 ± 1.1	34.66 ± 1.7
8	28.76 ± 1.2	31.32 ± 1.0
9	23.83 ± 1.0	29.51 ± 1.3

[a] IC_{50} values in the cells were for 24 h incubation.

dye; which showed the preferential mitochondria localization of compounds (Fig. 6). As reflected from the merged images, the yellow colour suggested cytoplasmic distribution of the internalized BODIPYs **8** and **9** in mitochondria and not in the cell nucleus. Pearson's correlation coefficient (PCC) method was used to estimate the extent of localization [35] which indicated significant mitochondrial localization of the BODIPYs. The preferred localization of neutral BODIPYs **8** and **9** within mitochondria could be attributed to the water soluble thio-hexose sugars linked to the BODIPYs. Above results, designate that the neutral water soluble BODIPYs (**8** and **9)** containing glucose and galactose units are capable of selectively targeting the mitochondria in live cells without inducing significant damage to cells. Also, easy synthesis of such BODIPY based probes can be explored further to develop NIR dyes for potential applications in *in-vivo* fluorescence imaging.

3. Conclusion

Simple, yet effective stepwise synthesis of water soluble thio-glycosylated BODIPYs is reported. These neutral thio-glycosylated BODIPYs were synthesized from the pentafluorophenyl dipyrromethane in four steps with reasonable yields. The BODIPYs exhibited significant cytotoxicities for HaCaT and HeLa cells making them potential candidate for anti-cancer treatment. The calculated IC_{50} values for BODIPYs were in the range of 23.83–48.61 μM in these cells. These BODIPYs are more active in HaCaT cells with IC_{50} values in between 23.83 and 38.15 μM. ROS generation study in HaCaT cells, revealed that thioglucosyl substituted BODIPYs has higher cellular uptake than the rest of the BODIPYs. Strong emission of thioglycosylated BODIPYs around 535 nm enabled us to probe subcellular localization by confocal microscopy. Selective mitochondrial localization of these neutral water soluble thioglycosylated BODIPYs makes them promising candidates for cancer treatment as theranostic agents.

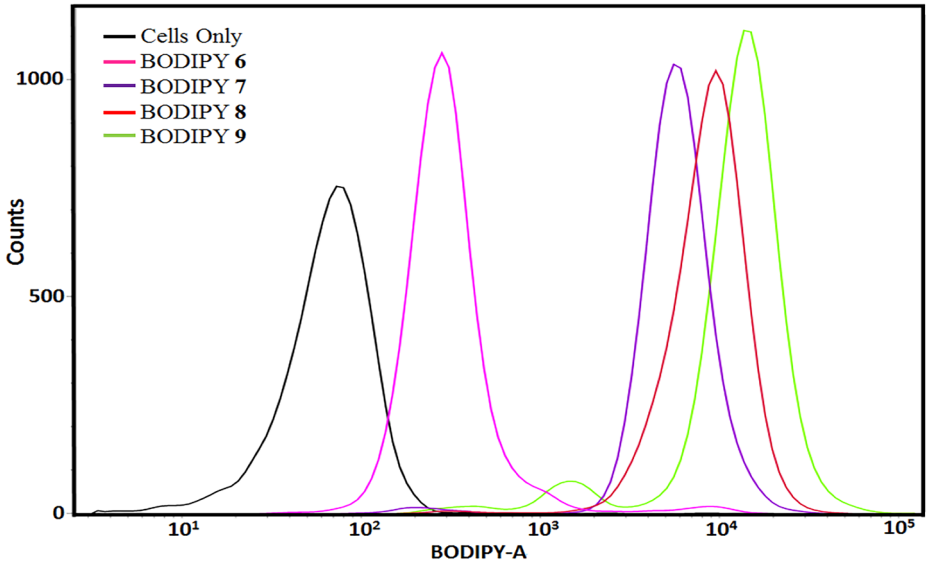

Fig. 5. Cellular uptake of BODIPYs **6–9** as obtained from flow cytometry after incubating with HaCaT cells.

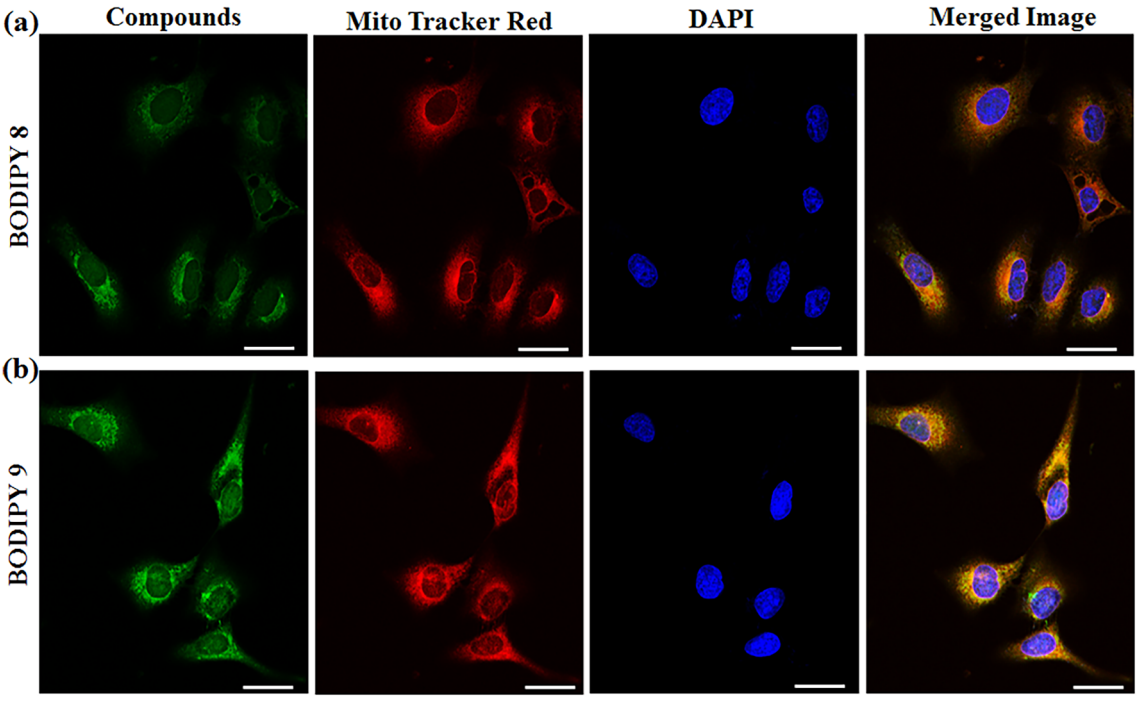

Fig. 6. Confocal microscopic images of BODIPYs **8** and **9** (10 μM) showing green emission in HaCat cells on 24 h incubation. Top and bottom rows are for BODIPYs **8** and **9**, respectively. Scale bar = 20 μm.

Acknowledgements

Financial support from SERB (EMR/2015/000779) Govt. of India, is greatly acknowledged. PK and VP thank IIT Gandhinagar for fellowship and infrastructural support.

Appendix A. Supplementary material

Supplementary data to this article can be found online at https://doi.org/10.1016/j.bioorg.2019.103139.

References

[1] D.J. Stephens, V.J. Allan, Science 300 (2003) 82–86.
[2] J. Rao, A. Dragulescu-Andrasi, H. Yao, Curr. Opin. Biotechnol. 18 (2007) 17–25.
[3] G. Ulrich, R. Ziessel, A. Harriman, Angew. Chem. Int. Ed. 47 (2008) 1184–1201.
[4] P.E. Kesavan, I. Gupta, Dalton Trans. 43 (2014) 12405–12413.
[5] P.E. Kesavan, S. Das, M.Y. Lone, P.C. Jha, S. Mori, I. Gupta, Dalton Trans. 44 (2015) 17209–17221.
[6] A. Kamkaew, S.H. Lim, H.B. Lee, L.V. Kiew, L.Y. Chung, K. Burgess, Chem. Soc. Rev. 42 (2013) 77–88.
[7] M. Vedamalai, D. Kedaria, R. Vasita, S. Mori, I. Gupta, Dalton Trans. 45 (2016) 2700–2708.
[8] R. Guliyev, S. Ozturk, E. Sahin, E.U. Akkaya, Org. Lett. 14 (2012) 1528–1531.
[9] M. Vedamalai, V.G. Krishnakumar, S. Gupta, S. Mori, I. Gupta, Sens. Actuat. B-Chem. 244 (2017) 673–683.
[10] M. Vedamalai, I. Gupta, Luminescence 33 (2018) 10–14.
[11] M. Vedamalai, D. Kedaria, R. Vasita, I. Gupta, Sens. Actuat. B-Chem. 263 (2018) 137–142.
[12] J. Nunnari, A. Suomalainen, Cell 148 (2012) 1145–1159.
[13] V. Gogvadze, S. Orrenius, B. Zhivotovsky, Semin. Cancer Biol. 19 (2009) 57–66.
[14] D.C. Wallace, Annu. Rev. Genet. 39 (2005) 359–407.
[15] H. Bugger, E.D. Abel, Cardiovasc. Res. 88 (2010) 229–240.
[16] A.M. Schaefer, M. Walker, D.M. Turnbull, R.W. Taylor, Mol. Cell. Endocrinol. 379 (2013) 2–11.
[17] J. Zielonka, J. Joseph, A. Sikora, M. Hardy, O. Ouari, J. Vasquez-Vivar, G. Cheng, M. Lopez, B. Kalyanaraman, Chem. Rev. 117 (2017) 10043–10120.
[18] B. Sui, S. Tang, A.W. Woodward, B. Kim, K.D. Belfield, Eur. J. Org. Chem. 2016 (2016) 2851–2857.
[19] B.A. Neto, J.R. Corrêa, R.G. Silva, RSC Adv. 3 (2013) 5291–5301.
[20] G.-Y. Pan, H.-R. Jia, Y.-X. Zhu, R.-H. Wang, F.-G. Wu, Z. Chen, ACS Biomater. Sci. Eng. 3 (2017) 3596–3606.
[21] A. Baracca, G. Sgarbi, G. Solaini, G. Lenaz, BBA-Bioenerg. 1606 (2003) 137–146.
[22] S. Rimpelová, T.s. Bříza, J. Králová, K. Záruba, Z.k. Kejík, I. Císařová, P. Martásek, T.s. Ruml, V. Král, Bioconjugate Chem. 24 (2013) 1445–1454.
[23] T. Gayathri, S. Karnewar, S. Kotamraju, S.P. Singh, ACS Med. Chem. Lett. 9 (2018) 618–622.
[24] T. Bura, R. Ziessel, Org. Lett. 13 (2011) 3072–3075.
[25] G. Fan, L. Yang, Z. Chen, Front. Chem. Sci. Eng. 8 (2014) 405–417.
[26] A.L. Nguyen, K.E. Griffin, Z. Zhou, F.R. Fronczek, K.M. Smith, M.G.H. Vicente, New J. Chem. 42 (2018) 8241–8246.
[27] N. Shivran, M. Tyagi, S. Mula, P. Gupta, B. Saha, B.S. Patro, S. Chattopadhyay, Eur. J. Med. Chem. 122 (2016) 352–365.
[28] X. Chen, L. Hui, D.A. Foster, C.M. Drain, Biochemistry 43 (2004) 10918–10929.
[29] W. Qin, M. Baruah, M. Van der Auweraer, F.C. De Schryver, N. Boens, J. Phys. Chem. A 109 (2005) 7371–7384.
[30] A.M. Courtis, S.A. Santos, Y. Guan, J.A. Hendricks, B. Ghosh, D.M. Szantai-kis, S.A. Reis, J.V. Shah, R. Mazitschek, Bioconjug. Chem. 25 (2014) 1043–1051.
[31] P. Skehan, R. Storeng, D. Scudiero, A. Monks, J. McMahon, D. Vistica, J.T. Warren, H. Bokesch, S. Kenney, M.R. Boyd, J. Natl. Cancer Inst. 82 (1990) 1107–1112.
[32] R. Diaz-Ruiz, M. Rigoulet, A. Devin, Biochim. Biophys. Acta 1807 (2011) 568–576.
[33] M.L. Macheda, S. Rogers, J.D. Best, J. Cell. Physiol. 203 (2005) 654–662.
[34] S. Rodriguez- Enriquez, A. Marin-Hernandez, J.C. Perez-Gallardo, R. Moreno-Sanchez, J. Cell. Physiol. 221 (2009) 552–559.
[35] H. Wang, J.A. Joseph, Free Radic. Biol. Med. 27 (1999) 612–616.
[36] N. Roopa, V. Kumar, M. Bhalla Kumar, Chem. Commun. 51 (2005) 15614–15628.
[37] S.C. Dodani, S.C. Leary, P.A. Cobine, D.R. Winge, C.J. Chang, J. Am. Chem. Soc. 133 (2011) 8606–8616.
[38] H. He, D.-W. Li, L.-Y. Yang, L. Fu, X.-J. Zhu, W.-K. Wong, F.-L. Jiang, Y. Liu, Scient. Rep. 5 (2015) 13543.
[39] Z. Yang, Y. He, J.-H. Lee, N. Park, M. Suh, W.-S. Chae, J. Cao, X. Peng, H. Jung, C. Kang, J.S. Kim, J. Am. Chem. Soc. 135 (2013) 9181–9185.
[40] T.A. Prime, M. Forkink, A. Logan, P.G. Finichiu, J. McLachlan, P.B.L. Pun, W.J.H. Koopman, L. Larsen, M.J. Latter, R.A.J. Smith, M.P. Murphy, Free Radic. Biol. Med. 53 (2012) 544–553.
[41] X. Zhang, Y. Xiao, J. Qi, J. Qu, B. Kim, X. Yue, K.D. Belfield, J. Org. Chem. 78 (2013) 9153–9160.
[42] M. Gao, F. Yu, H. Chen, L. Chen, Anal. Chem. 87 (2015) 3631–3638.
[43] T. Sun, X. Guan, M. Zheng, X. Jing, Z. Xie, ACS Med. Chem. Lett. 6 (2015) 430–433.